Benefits of an Advanced AC OPF Model in the Croatian Transmission Network

Karlo Šepetanc, Hrvoje Pandžić
Innovation Centre Nikola Tesla (ICENT) &
University of Zagreb Faculty of
Electrical Engineering and Computing
Zagreb, Croatia
karlo.sepetanc@fer.hr
hrvoje.pandzic@fer.hr

Tomislav Plavšić, Vladimir Valentić, Renata Rubeša
Croatian Transmission System Operator (HOPS)
Zagreb, Croatia
tomislav.plavsic@hops.hr
vladimir.valentic@hops.hr
renata.rubesa@hops.hr

Abstract—Modern transmission systems operation and planing problems involve computationally difficult optimizations. Transmission system operators forecast, monitor and manage power flows to ensure that the system always operates within permitted limits. This paper develops an AC Optimal Power Flow (AC OPF) algorithm intended to enhance numerical efficiency for commonly occurring cases in real-world transmission system networks. These systems include discrete devices, e.g. controllable transformer tap, generator automatic voltage control and variable shunt reactor (VSR), whose operational models are too computationally demanding for general nonlinear optimization. The developed algorithm divides the computational burden in two parts. The first part solves AC OPF with computationally demanding binary variables fixed to the initial power flow state, while the second part tries to find a better solution for fixed variables using more tractable AC OPF approximation. The efficiency of the approach is demonstrated on the Croatian transmission network and real operating data. The optimization succeeds to satisfy the initially exceeded operating constraints. Results also indicate that the direct approach that solves for all variables simultaneously using the exact nonlinear AC OPF model is computationally intractable for the considered cases.

Index Terms—AC Optimal power flow, voltage-var control, industrial transmission network

NOMENCLATURE

A. Sets and Indices

E	Tuple set of branches in forward orientation, indexed by (e, i, j).
N^{VC}	Set of automatic controlled buses, indexed by i and j.
NG^{VC}	Tuple set of automatic controlled buses and generators performing control at that bus, indexed by (i, k).
S	Sets of shunts, indexed by s.
τ	Set of time steps, indexed by t.
R	Set of infeasible automatic voltage control states, indexed by r.

B. Parameters

$\tau_e^\alpha, \tau_e^\beta$	Transformer tap magnitude coefficients.
b_s^α, b_s^β	Shunt susceptance coefficients.
$V_{t,i}^{\mathbf{point}}$	Generator automatic voltage control setpoint.
$\underline{Q}_k^{\mathbf{g}}, \overline{Q}_k^{\mathbf{g}}$	Generator minimum and maximum reactive power production.
$\underline{V}_i, \overline{V}_i$	Bus minimum and maximum voltage magnitude.
$x_{t,i,r}^{\mathbf{P\_up}}, x_{t,i,r}^{\mathbf{P\_dn}}$	Infeasible voltage control state memory.

C. Variables

$Q_{t,k}^{\mathrm{g}}$	Generator reactive power production.
$V_{t,i}$	Bus voltage.
$\tau_{t,e}, y_{t,e}^\tau$	Branch tap magnitude and integer switch state.
$b_{t,s}^{\mathrm{sh}}, x_{t,s}^{\mathrm{sh}}, y_{t,s}^{\mathrm{sh}}$	Shunt susceptance, binary and integer major and minor block switch states.
$x_{t,i}^{\mathrm{up}}, x_{t,i}^{\mathrm{dn}}$	Indicative binary variable for reached upper or lower limit of generator reactive power production.

1. INTRODUCTION

Optimal power flow (OPF) is a well studied optimization problem in power systems, first introduced in 1962 [1]. Its objective is to find an operating point that minimizes the cost of power generation while satisfying operating constraints and meeting demand. Implementation of the OPF algorithms in transmission system operators' control centers, for real-time and near real-time applications, generally faces serious challenges. The real-world OPF algorithms need to be fast, robust, easy to interpret, and with realistic values for control variables. Simplified models that rely on the DC approximation of power flows. e.g. [2], are not sufficiently accurate and in operating centers the systems operators need to rely on accurate AC representation of power flows. Not less important is a procedure for control variables adjustment, whether it is automatic or manual. As there are different cost functions usually applied for OPF algorithms in control centers, like security-constrained OPF (SCOPF) or standard volt-var control OPF (VVC OPF), it is also important to establish secure and reliable sequence for the running OPF to avoid overlapping and confusing the operating staff.

Authors in [3] evaluated the technical requirements for implementation of a centralized VVC function within an existing supervisory control and data acquisition or energy management systems. The challenges of the implementation are related to the limitations of the existing network model and mathematical modelling of network elements, input data, measurement quality and state estimation output reliability. In [4], the authors tested a coordinated real-time VVC algorithm on the IEEE 118-bus system in a simulated real-time environment. The results demonstrate system stability with new dispatch points and significant improvement in the system-wide voltage profiles as compared to an uncontrolled scenario. This has proved, according to the authors, that the developed algorithm is ready to move to the implementation phase. However, the authors did not consider generators' automatic voltage control commonly encountered in actual power systems. If the automatic voltage control is not controllable by the system operator, which can occur for example if the generator is in a neighbouring country or simply has fixed control settings, then the automatic voltage control model includes computationally difficult binary variables, as explained in Section 2 . In this paper, we address numerical tractability of the VVC OPF in real-world transmission system with generators' operating under the automatic voltage control.

The difficulty of solving AC OPF with integer variables arises from poor warm-start capabilities of interior-point algorithm used in general nonlinear solvers. Poor warm-start capabilities mean that each node in the branch-and-bound search tree is as difficult as the root node, or even more difficult if the node is infeasible, as the algorithm is also weak in infeasibility detection. In the literature, there are numerous AC OPF relaxations and approximations developed with the aim of improving numerical tractability of AC OPF with integer variables. Commonly used relaxation models are Jabr's second-order cone programming (SOCP) model [5] and Shor's semidefinite programming (SDP) model [6]. Jabr's SOCP model is well know to perform well for radial networks, but large errors occurs with meshed transmission networks. Shor's SDP model is know to be very computationally demanding and solvable in only rare dedicated SDP solvers. Linear approximation models, such as [7], generally have larger errors than the quadratic models and iterative solution refinements are required to decrease the error which can not be fully eliminated. The convex quadratic approximation in [9] has been shown to be of high accuracy for meshed transmission system networks in single iteration with numerical tractability on a par with other convex quadratic models. As such, we develop an algorithm that solves an industrial transmission system AC OPF problem using a both exact AC OPF model due to required accuracy and more tractable AC OPF approximation from [9] to improve on assumed fixed integer variables in the exact model. Ultimately, tractability results are compared to the direct approach that solves for all variables simultaneously using exact nonlinear AC OPF model.

Contribution of the paper consists of the following:
- We develop an algorithm for solving voltage-var control

AC OPF in transmission networks considering the generators' automatic voltage control.
- To prove its effectiveness, the algorithm is compared to the approach that solves for all variables simultaneously.

Rest of the paper is structured as follows. Section 2 mathematically states and explains the proposed algorithm. Case study section 3 is divided in two parts: the first part shows benefits for the system in terms of the achieved voltage magnitudes and active power losses. The second part compares computation time and objective function result of the developed algorithm with the approach that solves for all variables simultaneously. Section 4 provides relevant conclusions and guidelines for future work.

2 . MATHEMATICAL MODEL

The developed AC OPF Algorithm 1 for transmission networks has two parts. The first part, the Step 2, computes OPF under the assumption that no generator operating automatic voltage control changes its control state: i) from constant voltage (if the reactive power production at the initial power flow state is within the bounds); ii) constant reactive power production if the reactive power production is at the generators limit initially. The second part of the algorithm (Steps 3–6) addresses possible generators' voltage control state changes. It computes the OPF with control state as a variable. The difference between the first and the second part of the Algorithm is that the first part uses exact nonlinear polar OPF [8] so its solution is not susceptible to approximation or relaxation errors, while the second part uses convex polar second-order approximation (CPSOTA) AC OPF model [9], which is more efficient for computing computationally difficult binary variables associated with the generators' voltage control states. The final solution is always obtained from Step 2, i.e. the exact polar model, so it does not contain an OPF approximation. The second part of the Algorithm merely checks for more favourable voltage control states, which, if found, is used to initialize a new algorithm loop with new voltage magnitudes and reactive powers at the automatic voltage controlled nodes. The algorithm runs until no improvement in control states is found. The following paragraphs explain the models and the second part of the algorithm in more detail.

TSOs perform aftermarket checks of the system security and minimize active power losses. The two responsibilities are usually preformed separately. The $n - 1$ security is addressed by optimizing active power production and transversal control transformers. On the other hand, voltage magnitudes and losses are addressed by optimizing reactive power production, longitudinal control transformers and VSRs. In the context of this paper, we consider the VVC OPF. The goal of VVC is to bring voltage magnitudes within the nominal range and to minimize system losses (in terms of MWh) or their expenses (in monetary units). The objective function (1.1) represents the TSO's perspective, which is to minimize active power losses.

$$\text{Min} \sum_{(e,i,j) \in E} (P_{t,e,i,j} + P_{t,e,j,i}) \qquad (1.1)$$

Algorithm 1 AC OPF

1: **repeat**
2:     Exact polar model
- control variables: controllable generators, transformer taps and VSRs;
- fixed V or Q at automatic voltage controlled nodes.

3:     **repeat**
4:         Presolve [9]
- if feasible, expands the list of quadratic constraints that are likely to cause relaxation errors;
- if infeasible, forbids current automatic voltage control states combination.

5:         Convex polar second-order approximation [9]
- control variables: controllable generators and automatic voltage control states;
- fixed transformer taps and VSRs;
- expands the list of quadratic constraints that are likely to cause relaxation errors with constraints that resulted in relaxation errors.

6:     **until** No relaxation errors and feasible presolve
7: **until** No automatic voltage control state change

Equation (1.2) defines tap magnitude $\tau_{t,e}$ of tap changer transformers controllable by the TSO. It is a variable occurring in the denominator of the power flow equations. In the second part of Algorithm 1 it is always a parameter to retain the convex quadratic optimization form. In the first part, it is a variable if the transformer is controllable and a parameter if it is not. $y^{\tau}_{t,e}$ is an integer variable whose values range from the most negative switch position to the maximum positive one. Equation (1.3) defines the controllable VSRs' susceptance. VSRs consist of major switchable segments and many minor. $x^{\mathrm{sh}}_{t,s}$ represents a binary variable indicating if a major segment is turned on and $y^{\mathrm{sh}}_{t,s}$ is an integer variable indicating how many minor susceptance segments are switched on. In case a VSR is not controllable, its suscenpance is treated as a constant.

$$\tau_{t,e} = \boldsymbol{\tau}^{\alpha}_e + \boldsymbol{\tau}^{\beta}_e \cdot y^{\tau}_{t,e}, \quad \forall t, e \qquad (1.2)$$

$$b^{\mathrm{sh}}_{t,s} = \boldsymbol{b}^{\alpha}_s \cdot x^{\mathrm{sh}}_{t,s} + \boldsymbol{b}^{\beta}_s \cdot y^{\mathrm{sh}}_{t,s}, \quad \forall t, s \qquad (1.3)$$

Generators' automatic voltage control has a discrete characteristic displayed in Fig. 1. Either the generator's reactive power is within the production bounds and maintains the voltage magnitude constant or the reactive power has already reached the limit so the voltage magnitude drifts away from the control set value $V^{\mathbf{point}}_{t,i}$. Equations (1.4)–(1.7) define the three segments in the figure. Binary indicator variable $x^{\mathrm{up}}_{t,i}$ forces the reactive power production to the maximum value and voltage magnitude to be lower or equal than the control set value if equal to one. If binary variable $x^{\mathrm{dn}}_{t,i}$ takes value one, it analogously forces the generator's reactive power to the minimum value and voltage to be greater of equal than the control set value. If both binary variables are zero,

then the corresponding bus voltage magnitude is equal to the control set point and reactive power is within the production bounds. Both binary variables can not have value one since that is an infeasible combination, i.e. reactive power can not be simultaneously at the upper and at the lower bound.

$$V_{t,i} - \boldsymbol{V}^{\mathbf{point}}_{t,i} \leqslant (\overline{\boldsymbol{V}}_i - \boldsymbol{V}^{\mathbf{point}}_{t,i}) \cdot x^{\mathrm{up}}_{t,i}, \quad \forall t, i \in N^{\mathrm{VC}} \quad (1.4)$$

$$\boldsymbol{V}^{\mathbf{point}}_{t,i} - V_{t,i} \leqslant (\boldsymbol{V}^{\mathbf{point}}_{t,i} - \underline{\boldsymbol{V}}_i) \cdot x^{\mathrm{dn}}_{t,i}, \quad \forall t, i \in N^{\mathrm{VC}} \quad (1.5)$$

$$Q^{\mathrm{g}}_{t,k} - \underline{\boldsymbol{Q}}^{\mathbf{g}}_k \leqslant (\overline{\boldsymbol{Q}}^{\mathbf{g}}_k - \underline{\boldsymbol{Q}}^{\mathbf{g}}_k) \cdot (1 - x^{\mathrm{up}}_{t,i}), \quad \forall t, (i,k) \in NG^{\mathrm{VC}} \quad (1.6)$$

$$\overline{\boldsymbol{Q}}^{\mathbf{g}}_k - Q^{\mathrm{g}}_{t,k} \leqslant (\overline{\boldsymbol{Q}}^{\mathbf{g}}_k - \underline{\boldsymbol{Q}}^{\mathbf{g}}_k) \cdot (1 - x^{\mathrm{dn}}_{t,i}), \quad \forall t, (i,k) \in NG^{\mathrm{VC}} \quad (1.7)$$

The second part of the algorithm consists of CPSOTA AC OPF [9] in combination with a presolve also described in paper [9]. CPSOTA is a local AC OPF model for an operating point consisting of the voltage magnitude $V_{t,i}$ and angle $\boldsymbol{\theta}^{\mathbf{op}}_{t,i}$, which is here computed in the first part of the algorithm. The presolve (Step 4 in Algorithm 1) selects the relaxed quadratic constraints likely to cause relaxation errors for the operating point by evaluating constraint marginals and replaces them with linear equality. It runs for the operating point determined in the first part of Algorithm 1 and for the current fixed automatic voltage control states from either the polar model (Step 2 in Algorithm 1) or the CPSOTA (Step 4 in Algorithm 1), whichever is run beforehand in the algorithm flow chart. The presolve does not have any discrete variables so it is computationally tractable despite it being nonconvex. If it finds that the current automatic control state determined by the previous run of CPSOTA AC OPF is infeasible, which can occur since the CPSOTA is an approximation, it adds a constraint (1.8) that prevents this combination from occurring again. Parameters $x^{\mathbf{P\_up}}_{t,i,r}$ and $x^{\mathbf{P\_dn}}_{t,\bar{i},r}$ represent the determined infeasible automatic voltage control state combination r. In the first inner loop, r is always an empty set of states which means that there is no constraint (1.8) for the first pass. Described part of the algorithm runs in loops until the presolve is feasible and no CPSOTA relaxation errors occur which ensures accuracy.
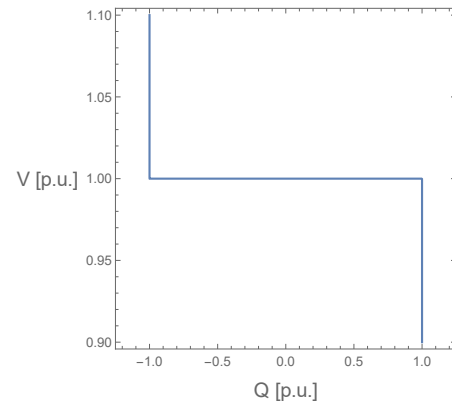
Fig. 1: Generators' automatic voltage control operation diagram.

$$\sum_{\substack{t,i\in N^{\mathrm{VC}}\\:\boldsymbol{x}_{t,i,r}^{\mathbf{P\_up}}=1}}(1-x_{t,i}^{\mathrm{up}}) + \sum_{\substack{t,i\in N^{\mathrm{VC}}\\:\boldsymbol{x}_{t,i,r}^{\mathbf{P\_up}}=0}}x_{t,i}^{\mathrm{up}} + \sum_{\substack{t,i\in N^{\mathrm{VC}}\\:\boldsymbol{x}_{t,i,r}^{\mathbf{P\_dn}}=1}}(1-x_{t,i}^{\mathrm{dn}}) + \sum_{\substack{t,i\in N^{\mathrm{VC}}\\:\boldsymbol{x}_{t,i,r}^{\mathbf{P\_dn}}=0}}x_{t,i}^{\mathrm{dn}} \geqslant 1, \quad \forall r$$

(1.8)

3. CASE STUDY

The transmission system network data includes Croatia and major nodes of the neighbouring countries for four time periods on 7 December, 2020: 15:05–15:15, 16:10–16:20, 17:20–17:30 and 18:10–18:20 CET. At these timestamps generally high voltage magnitudes were observed. Croatian transmission network system was chosen primarily because there is a real-time VVC OPF already functional in the Croatian transmission system operator's national control center, so it is beneficial to investigate if there is a possibility to improve already very reliable and efficient OPF tool. Croatian transmission network has an unusual topology on the 400 kV level without a closed ring through its own system (visualization of the system is available at [10]), what makes it difficult to optimise voltages and gain cost function benefits, adjusting the control variables solely in the Croatian transmission network system. The network has 411–414 buses (110 kV, 220kV and 400 kV nodes), depending on the time period and data is in p.u. or dimensionless. Each time period consists of the initial state, and the final state 10 minutes after the initial one, which is considered sufficient for a system to react to the TSO's control. The optimization is performed for the initial state, but since every control has a time delay, the optimization results are displayed for the final state. The initial state is real measured data and the final state is simulated system power flow response, based also on real measurement data, but with changed control variables. The case study is divided in two parts. The first part demonstrates the benefits of optimization on voltage magnitudes and changes in active power losses. The second part compares the results in terms of the solution time and achieved objective function of the proposed algorithm and the direct approach where the exact polar model is used to solve for all variables concurrently.

1) Voltage magnitudes and active power losses:

Tables I–IV show voltage magnitudes for the network at different times for the select high-voltage buses in Croatia. Red colored voltage magnitudes V^{init} and V^{noopt} represent the observed overvoltages at the initial state and the final state without the TSO's control intervention. Results in the last column show the simulated voltage magnitudes V^{noopt} for the system at the final state with the TSO's actions determined based on the optimization of the initial system state. In all cases, overvoltages are removed by the optimization despite the uncertain realization of the 10-minutes timespan. Comparing the final times with and without optimization, the optimization case resulted in higher losses despite the objective function being the loss minimization. This occurs since the optimization needs to lower voltages to satisfy the operation constraints. Lower voltage magnitudes lead to higher active power losses.

TABLE I: Voltage magnitudes for 15:05–15:15 time period for the initial state and the final state with and without control actions.

Bus ID	Nominal voltage (kV)	V^{max} (p.u.)	V^{init} (p.u.)	V^{noopt} (p.u.)	V^{opt} (p.u.)
60032	400	1.05	1.05023	1.04868	1.04423
60066	400	1.05	1.05141	1.04729	1.03994
60129	400	1.05	1.05117	1.04805	1.04516
60150	400	1.05	1.05625	1.05309	1.04795
60015	220	1.11818	1.0974	1.09649	1.10841
60067	220	1.11818	1.08951	1.08553	1.06711
60071	220	1.13636	1.10589	1.10214	1.08867
60090	220	1.11818	1.08637	1.08242	1.06442
60109	220	1.11818	1.10897	1.10436	1.08758
60145	220	1.13636	1.14109	1.13881	1.13532
60151	220	1.11818	1.11163	1.10807	1.09758
60158	220	1.11818	1.08676	1.08502	1.06332
60170	220	1.11818	1.11434	1.1064	1.08459
Losses (MW):			31.38	33.27	34.14

TABLE II: Voltage magnitudes for 16:10–16:20 time period for the initial state and the final state with and without control actions.

Bus ID	Nominal voltage (kV)	V^{max} (p.u.)	V^{init} (p.u.)	V^{noopt} (p.u.)	V^{opt} (p.u.)
60032	400	1.05	1.04786	1.04676	1.04427
60066	400	1.05	1.0459	1.0464	1.04034
60129	400	1.05	1.04595	1.0454	1.04402
60150	400	1.05	1.05051	1.04896	1.0464
60015	220	1.11818	1.09493	1.08874	1.08977
60067	220	1.11818	1.08482	1.08752	1.0706
60071	220	1.13636	1.099	1.1001	1.08634
60090	220	1.11818	1.08171	1.08408	1.06836
60109	220	1.11818	1.10309	1.10539	1.09212
60145	220	1.13636	1.14012	1.13872	1.13446
60151	220	1.11818	1.10498	1.09928	1.09082
60158	220	1.11818	1.08441	1.0865	1.06818
60170	220	1.11818	1.10276	1.10701	1.09173
Losses (MW):			33.44	34.72	34.76

TABLE III: Voltage magnitudes for 17:20–17:30 time period for initial state and final state with and without control actions.

Bus ID	Nominal voltage (kV)	V^{max} (p.u.)	V^{init} (p.u.)	V^{noopt} (p.u.)	V^{opt} (p.u.)
60032	400	1.05	1.04871	1.04843	1.04581
60066	400	1.05	1.06264	1.06193	1.04956
60129	400	1.05	1.05058	1.05044	1.04825
60150	400	1.05	1.05245	1.0527	1.04915
60015	220	1.11818	1.08872	1.08896	1.09017
60067	220	1.11818	1.09757	1.0943	1.05565
60071	220	1.13636	1.10508	1.10454	1.08303
60090	220	1.11818	1.09316	1.08969	1.05221
60109	220	1.11818	1.11276	1.11156	1.08564
60145	220	1.13636	1.13252	1.13225	1.1285
60151	220	1.11818	1.10385	1.10341	1.09037
60158	220	1.11818	1.0942	1.09007	1.04767
60170	220	1.11818	1.11386	1.11359	1.09191
Losses (MW):			34.23	33.76	34.14

TABLE IV: Voltage magnitudes for 18:10–18:20 time period for initial state and final state with and without control actions.

Bus ID	Nominal voltage (kV)	V^{max} (p.u.)	V^{init} (p.u.)	V^{noopt} (p.u.)	V^{opt} (p.u.)
60032	400	1.05	1.04949	1.04908	1.04587
60066	400	1.05	1.05804	1.05274	1.04569
60129	400	1.05	1.05145	1.05004	1.04859
60150	400	1.05	1.05424	1.05319	1.04933
60015	220	1.11818	1.09156	1.08671	1.09209
60067	220	1.11818	1.07984	1.07268	1.05114
60071	220	1.13636	1.10491	1.10185	1.07115
60090	220	1.11818	1.0769	1.07001	1.04891
60109	220	1.11818	1.10287	1.09748	1.07938
60145	220	1.13636	1.12953	1.13185	1.11852
60151	220	1.11818	1.10475	1.10297	1.0849
60158	220	1.11818	1.07743	1.07054	1.04271
60170	220	1.11818	1.11438	1.11275	1.07319
	Losses (MW):		33.71	36.07	36.94

2) Computation time and objective function:

The proposed algorithm is compared to the direct approach where all variables are concurrently determined using the exact nonlinear polar AC OPF [8]. All nonlinear and mixed-integer nonlinear models were solved using Knitro, while all mixed-integer quadratic models were solved using FICO Xpress, all on a PC laptop with i7-8565U CPU. Simulation results are displayed in Table V for the initial times. *Losses*, *MIP gap* and *Comp. time Alg. 1 part 1* columns refer to the first part of the algorithm and for the solution of the concurrent solve. The last two columns refer to the second part of the algorithm. Out of the four presented cases, the concurrent solve solves only the case at time 16:10. However, its solution is suboptimal, i.e. worse than achieved with the proposed algorithm, despite 0 reported MIP gap. This can occur due to nonconvexity of the model. For nonconvex models, the branch-and-bound technique can not guarantee optimality since individual nodes that the solver solves also can not guarantee optimality. Using the proposed approach, in all cases zero MIP gap solution was found. The maximum computation time for the first part was 126 seconds. The second part of the algorithm attempts to confirm or improve the current solution. For 16:10 time instance, the second part confirmed that the initial assumption for automatic voltage control states is optimal. For other cases it reached the imposed computation time limit of 30 minutes before finding a better solution. The computation time is long due to required low mip gap (0%) and large test network. The optimization could in principle run indefinitely due to exponential worst case branch and bound search tree complexity. Computation time limit is imposed to avoid stalled optimization. However, despite the reached time limit, all cases have a solution since the first part computed successfully.

4 . CONCLUSION

The proposed case study shows the importance of dividing difficult problems into easier ones. Binary variables are computationally demanding for nonlinear solvers, which is why the proposed algorithm outperforms the concurrent optimization of all variables. The second part of the algorithm attempts to improve the assumption on the values of the fixed difficult

binary variables in the first part. It confirms the assumption in one case and finds no better solution in the other three cases. The optimization was performed on Croatian the transmission network and has brought it withing the operating limits in all cases. The achieved losses were higher than without optimization, however, this is expected since voltage magnitudes were decreased to remove overvoltages. Future research will be focused on further improving the numerical tractability.

REFERENCES

[1] J. Carpentier, "Contribution a l'etude du dispacting economique," *Bull. Soc. Francaise des Electriciens*, vol. 3, pp. 431–447, 1962.
[2] Y. Dvorkin, P. Henneaux, D. S. Kirschen and H. Pandžić, "Optimizing Primary Response in Preventive Security-Constrained Optimal Power Flow," *IEEE Systems Journal*, vol. 12, no. 1, pp. 414–423, March 2018.
[3] R. Rubeša, M. Rekić, I.Ivankovic and N. Mandić, "Evaluation of Requirements for Volt/Var Control Implementation in Transmission Grid," *IEEE EUROCON 2019–18th International Conference on Smart Technologies*, Novi Sad, Serbia, 2019, pp. 1–6.
[4] M. Ghosal *et al.*, "Real-time Simulation of Coordinated Sub-Transmission Volt-Var Control Tool under High Distributed PV Penetration," *2020 IEEE Power & Energy Society Innovative Smart Grid Technologies Conference (ISGT)*, Washington, DC, USA, 2020, pp. 1–5.
[5] R. A. Jabr, "Radial distribution load flow using conic programming," *IEEE Trans. Power Syst.*, vol. 21, no. 3, pp. 1458–1459, Aug. 2006.
[6] X. Bai, H. Wei, K. Fujisawa and Y. Wang, "Semidefinite programming for optimal power flow problems," *Int. J. Elec. Power Energy Syst.*, vol. 30, no. 6, pp. 383–392, July 2008.
[7] Z. Yang, H. Zhong, A. Bose, T. Zheng, Q. Xia and C. Kang, "A Linearized OPF Model With Reactive Power and Voltage Magnitude: A Pathway to Improve the MW-Only DC OPF," *IEEE Trans. Power Syst.*, vol. 33, no. 2, pp. 1734–1745, March 2018.
[8] S. Frank and S. Rebennack, "An introduction to optimal power flow: Theory, formulation, and examples," *IIE Transactions*, vol. 48, no. 12, pp. 1172–1197, 2016.
[9] K. Šepetanc and H. Pandžić, "Convex Polar Second-Order Taylor Approximation of AC Power Flows: A Unit Commitment Study," *IEEE Trans. Power Syst.*, vol. 36, no. 4, pp. 3585–3594, July 2021.
[10] Croatian Transmission System Operator – HOPS. [Online]. Available: www.hops.hr/en/system-scheme. [Accessed: 12-Feb-2023].

TABLE V: Computation time and losses for the proposed Alg. 1 and concurrent exact nonlinear polar model.

Time	Approach	Losses (MW)	MIP gap (%)	Comp. time Alg. 1 part 1 (s)	Result Alg. 1 part 2	Comp. time Alg. 1 part 2 (s)
15:05	Alg. 1	32.35	0	126	No improvement	1800
	Concurrent	No solution		1800	/	/
16:10	Alg. 1	33.32	0	0.2	Confirmed	37
	Concurrent	33.70	0	1.3	/	/
17:20	Alg. 1	34.51	0	1.4	No improvement	1800
	Concurrent	No solution		1800	/	/
18:10	Alg. 1	34.54	0	63	No improvement	1800
	Concurrent	No solution		1800	/	/